

Measurement of x-ray coherence using two-beam interferometer with prism optics

Yoshio Suzuki^{a)}

Japan Synchrotron Radiation Research Institute (JASRI), SPring-8, Mikazuki, Hyogo 679-5198, Japan

(Received 13 November 2003; accepted 22 December 2003; published 16 March 2004)

Two-beam x-ray interferometer using prism optics has been developed and applied to measurement of spatial coherence. Two-beam interferometry is made possible by using an x-ray prism as the beam deflector. A portion of the x-ray beam is deflected by the prism, and superimposed on the direct beam. This wavefront-dividing interferometer is essentially the same as well-known Fresnel's mirror experiment in visible light optics. Quantitative analysis of spatial coherence can be performed by measuring visibility of interference fringes. The experiment has been done at the undulator beamline 20XU of SPring-8. The measured visibility at an x-ray wavelength of 1 Å agrees well with theoretical value. Spatially coherent area larger than 0.5 mm was confirmed by analyzing the visibility of fringes. © 2004 American Institute of Physics. [DOI: 10.1063/1.1651640]

I. INTRODUCTION

A simple optics for x-ray interferometer has recently been studied,¹ and its preliminary applications to x-ray imaging have been reported.^{1,2} This interferometer consists of a single prism, and works the same as Lloyd's mirror interferometer. Therefore, the visibility of the interference fringe is a direct method of determining the degree of coherence. Many methods of coherence measurement have been proposed and used to characterize coherent properties in short wavelength regions, namely, Young's two-slit experiments,³⁻⁶ analysis of interference fringes in in-line hologram,⁷ use of a Bonse-Hart crystal interferometer,⁸ the direct measurement of x-ray emittance with crystal collimators,⁹ a two-beam interferometer with mirror optics,¹⁰ Fresnel's biprism optics,¹¹ and the intensity correlation method.^{12,13} Young's double-slit method has also been used to measure the spectrum of extreme-ultraviolet radiation.⁶ Quite recently, a method called uniformly redundant array (an extension of Young's double-slit method) has been developed, and used to measure the spatial coherence of hard x-ray undulator radiation.¹⁴ Of all of them, in the hard x-ray region, the intensity correlation method has given the best quantitative results¹³ to characterize third-generation synchrotron light sources.

Transversal coherent area is defined by $\lambda L/S$ for chaotic sources,^{15,16} where λ is the wavelength of x rays, L is the source to observation point distance, and S is the linear dimension of the x-ray source. Spontaneous emission of synchrotron radiation can be regarded as thermal radiation (essentially the same as blackbody radiation). Typical source size of third-generation synchrotron radiation source is smaller than 100 μm vertically, and smaller than 1 mm horizontally. The distance between the source point and experimental station is usually 50 m, and sometimes longer than 200 m. Therefore, the spatially coherent area at the experimental station is much larger than 100 μm in vertical direc-

tion. For example, by using a pseudopoint source defined by a pinhole, a maximum coherent area of about 1 mm is considered to be achieved at the beamline 20XU of SPring-8. However, the coherent properties of x-ray beams have never been characterized quantitatively.

In this article, a method of quantitative measurement of spatial coherence is described, and experimental results for 1 Å x rays are shown. The optical system is a kind of wavefront-dividing interferometer with a prism. A portion of the x-ray beam is refracted by passing through the prism, and the deflected beam is superimposed on the direct beam. The interference fringe is formed on the area where the beam overlaps. The degree of coherence is simply determined by measuring the visibility of interference fringes as changing the fringe spacings.

II. EXPERIMENTAL SETUP

Schematic diagram of the experimental setup is shown in Fig. 1. The experiment has been done at the beamline 20XU of SPring-8. A planar-type 173 pole undulator installed in the 8 GeV electron storage ring of SPring-8 is used as an x-ray source. The magnetic period of the undulator is 26 mm, and the maximum K value is 2.1. The stored electron beam current was 90–60 mA during the experiment. The undulator radiation is monochromatized by passing through a liquid-nitrogen-cooling Si 111 double crystal monochromator located 45 m from the source point. Both the first and second crystals of the monochromator are cooled by liquid-nitrogen, and kept at the same temperature in order to achieve fixed-exit-beam conditions. The experimental station is located about 245 m from the source point. A precise cross slit is placed in the beamline downstream from the crystal monochromator in order to control spatial coherence. The distance from the cross slit to the experimental station is 195 m, and the slit works as a pseudopoint source for the interference experiment. Three cross-slits with openings of 18 $\mu\text{m} \times 19 \mu\text{m}$, 51 $\mu\text{m} \times 50 \mu\text{m}$, or 103 $\mu\text{m} \times 105 \mu\text{m}$ can be selected by a linear translation feedthrough. The dimensions of the slits

^{a)}Electronic mail: yoshio@spring8.or.jp

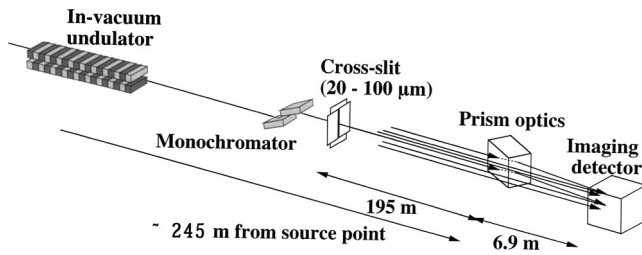


FIG. 1. Schematic diagram of experimental setup at beamline 20XU of SPring-8.

was measured by monitoring the transmission images at an x-ray energy of 18 keV. No optical elements, except for the crystal monochromator and the slit, are placed between the light source and the interferometer. There is only a Kapton vacuum window with a thickness of 125 μm at the entrance point of the experimental hutch. The cross-slit is located downstream from the monochromator. Therefore, when the spatial coherence is defined by the cross-slit, vibration or deformation of the monochromator crystals does not affect the spatial coherence.

The spatially coherent area A is defined by $A = \lambda L/S$, as previously mentioned. Under the present experimental conditions $\lambda = 1 \text{ \AA}$ and $L = 195 \text{ m}$. When a slit opening of $S = 19 \text{ μm}$ is selected, the transversal coherent area is calculated to be 1 mm. The monochromaticity ($\Delta\lambda/\lambda$) of the beam is about 10^{-4} . Therefore the longitudinal (temporal) coherent length defined by $\lambda^2/\Delta\lambda$ is about 1 μm at a wavelength of 1 Å. This value is sufficient for the present experiment.

The “x-ray prism” is a cube of acrylic resin, 20 mm in each dimension. The prism is placed on a rotation stage, and the deflection angle of the beam is adjusted by changing the angle of incidence onto the prism. As shown in Fig. 2, when a rectangular prism is used, the deflection angle $\Delta\theta$ is determined by the glancing angle to the prism surface θ as follows:

$$\Delta\theta = \delta / \tan(\theta),$$

where δ is the refractive index decrement from unity, as $n = 1 - \delta$. According to free-electron approximation, δ can be estimated with the well-known formula

$$\delta \sim 1.35 \times 10^{-6} \rho \lambda^2.$$

Therefore, δ is 1.62×10^{-6} for acrylic resin [density (ρ) = 1.2] at an x-ray wavelength of 1 Å. The deflection angle is smaller than a few μrad under normal incidence conditions.

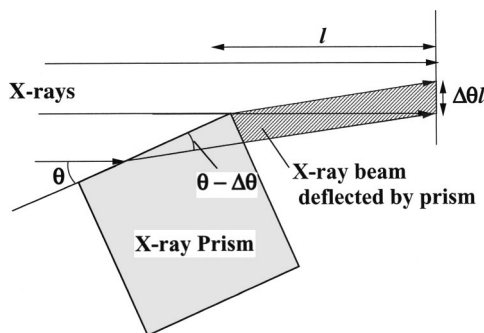


FIG. 2. Optical system for two-beam interferometer with x-ray prism.

However, it can be enhanced by choosing grazing incidence conditions. When θ is 2°, for example, the deflection angle becomes 46 μrad. Under these grazing incidence conditions for a rectangular prism, beam deflection at the exit boundary is negligibly small, and the deflection angle is determined only at the entrance surface. The details on the prism optics have already been described in a previous article.¹

As shown in Fig. 2, the beam-overlapping region is expressed by $\Delta\theta l$, and the fringe spacing d is written as $d = \lambda/\Delta\theta$, where l represents the distance between the prism and image plane. Under the present experimental conditions, $l = 6.9 \text{ m}$, and $\lambda = 1 \text{ \AA}$. Therefore the width of the interference region is predicted to be 320 μm, and the fringe spacing is 2.2 μm at a glancing angle of 2°. The interference area and fringe spacing can be controlled by rotating the prism. The visibility of the fringe (degree of coherence) is defined as

$$\gamma = (I_{\max} - I_{\min}) / (I_{\max} + I_{\min}),$$

where I_{\max} and I_{\min} are the maximum and minimum intensities of interference patterns, respectively. In the present experimental setup, the distance L ($= 195 \text{ m}$) is much longer than l ($= 6.9 \text{ m}$). Therefore, the visibility can be expressed by the following formula:^{15,16}

$$\gamma = \sin(\pi \Delta\theta l S / \lambda L) / (\pi \Delta\theta l S / \lambda L).$$

γ can be rewritten using the coherent area C ($= \lambda L/S$) and beam overlap B ($= \Delta\theta l$),

$$\gamma = \sin(\pi B/C) / (\pi B/C).$$

The above expression is valid when temporal coherence is sufficiently high to observe interference fringes. The maximum optical path difference is $\Delta\theta^2 l$. Under the present experimental conditions, $\Delta\theta < 10^{-4}$ rad, and $l = 6.9 \text{ m}$, the maximum path difference is shorter than 70 nm. That is sufficiently shorter than the longitudinal coherent length (1 μm) derived from monochromaticity. Therefore, the absolute value of the complex degree of spatial coherence is simply equal to γ .¹⁶ In this experiment, distance l is fixed, and the beam overlap is varied by changing the beam deflection angle $\Delta\theta$, i.e., by changing the fringe spacing $\lambda/\Delta\theta$.

Transmissivity of the prism is also significant in the interference experiment. The intensity ratio of the two beams should be near 1:1 in order to obtain the high visibility of interference fringes. The absorption coefficient of acrylic resin is 1.97 cm^{-1} at an x-ray wavelength of 1 Å. Therefore, visibility is suppressed by absorption loss through the prism. However, the absorption is usually negligible, except with thick prisms and under extreme grazing incidence conditions. The absorption effect can also be corrected by taking transmissivity into account. This correction is only required under extreme grazing incidence conditions (usually $\theta < 2^\circ$).

The interference images were recorded with an x-ray imaging detector, zooming tube (Hamamatsu Photonics, Hamamatsu, Japan, C5333). It consists of a thin photocathode (CsI, 2000-Å thick) and electromagnetic lens system, microchannel plate, phosphor screen, optical relay lens, and a cooled charge-coupled device (CCD). The CCD has 1000 × 1018 pixels, and each pixel is 12 μm × 12 μm. The x-ray image is converted to a photoelectron image by the photo-

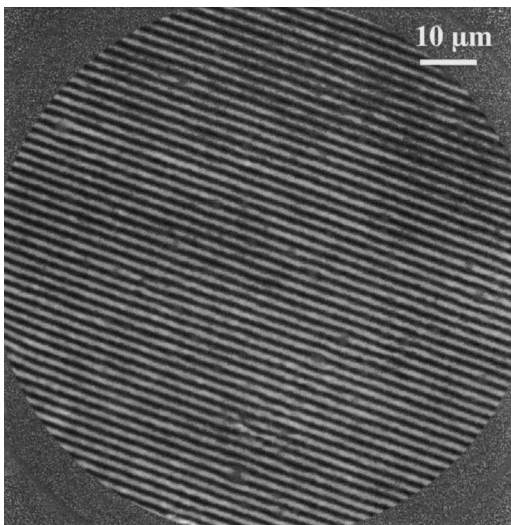


FIG. 3. Typical interference fringe patterns measured at an x-ray wavelength of 1 Å. Beam deflection angle: $\Delta\theta=44 \mu\text{rad}$. Slit dimensions: $18 \mu\text{m}\times 19 \mu\text{m}$. Measured fringe spacing is $2.3 \mu\text{m}$. Beam overlap is $300 \mu\text{m}$. Exposure time is 60 s.

cathode, and the photoelectron image is magnified by the electromagnetic lens system. The magnified image is amplified by the microchannel plate, and converted to a visible light image at the phosphor screen. Finally, the optical image is measured with the CCD camera. The electromagnetic lens was operated at a magnification of 230, and the optical relay lens with a magnification of 0.5 was used. Therefore, the effective dimension of a unit pixel was $0.1 \mu\text{m}\times 0.1 \mu\text{m}$. The point-spread-function (PSF) and modulation-transfer-function (MTF) of the zooming tube has already been measured at SPring-8, and the full-width at half-maximum of the PSF was measured to be $0.7 \mu\text{m}$ at an x-ray energy of 8 keV.¹⁷

III. RESULTS AND DISCUSSION

An example of interference fringes at a beam deflection angle of $44 \mu\text{rad}$ is shown in Fig. 3. Periodic interference fringes with a period of $2.3 \mu\text{m}$ can clearly be observed. Visibilities of the fringes are measured as changing the fringe period and the size of slit that defines the source dimensions. The results are shown in Fig. 4. The measured visibility data

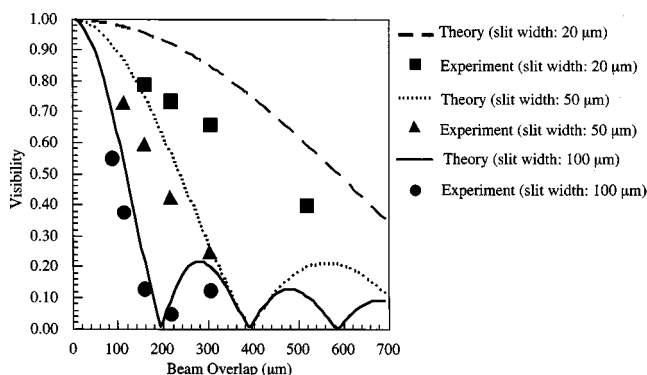


FIG. 4. Visibility of interference fringes. Solid squares, circles, and triangles represent experimental data, and solid line, dotted line and dashed line are respective theoretical curves for source size of 100, 50, and $20 \mu\text{m}$.

TABLE I. Observed source size by least-mean-square curve fit.

Cross slit dimensions	Observed source dimension (μm)
$18 \mu\text{m}\times 19 \mu\text{m}$	28
$51 \mu\text{m}\times 50 \mu\text{m}$	57
$103 \mu\text{m}\times 105 \mu\text{m}$	112

are corrected by the MTF of the imaging detector. The observed visibility agrees well with the theoretical value. The source dimensions derived from measured interference fringes with the least-mean-square curve fit are listed in Table I. For example, a measured slit width of $27 \mu\text{m}$ is obtained for a $19 \mu\text{m}$ slit. The measured slit width agrees with the geometrical source size within an accuracy of about $20 \mu\text{m}$. In this experiment, the distance between the x-ray source and interferometer is 195 m. Therefore, it is concluded that the two-beam x-ray interferometer has an angular resolution of about 100 nano-radian (~ 0.02 arc sec).

The angular resolution of telescope with rectangular aperture is determined as $0.5 \lambda/A$, where A is the aperture of telescope. This angular resolution is consistent with the resolution determined by the maximum aperture of the interferometer (0.5 mm).

However, there is still a slight difference between the measured visibility and theoretical value. The measured amplitude is always smaller than the theoretical. It is supposed that the difference might be due to the compensation of spatial resolution of the detector. Although the x-ray energy is 12.4 keV in this experiment, the MTF of the imaging detector used for data correction has been measured at 8 keV. It has also been found that the spatial resolution of the zooming tube slightly depends on the x-ray energy. The width of the PSF at 82 keV is estimated to be about $1.2 \mu\text{m}$. Therefore, for more precise analysis, the PSF of the imaging detector should be measured at the x-ray energy that is used in the interference experiment.

At present, it is difficult to measure the vertical beam size of electron orbit of the SPring-8 storage ring, because the x-ray beam is disturbed by vibration of the monochromator. The vibration of monochromator crystal is estimated to be about 0.7 arc sec ($\sim 3.5\times 10^{-6}$ rad). As the distance between the source point and the monochromator is 45 m, the source image is estimated to broaden by about $320 \mu\text{m}$ due to the vibration of the monochromator crystal. The vibration of the crystal need to be less than $0.5 \mu\text{rad}$ in order to measure the source size smaller than $40 \mu\text{m}$. Deformation of the crystal may also be a problem. However, when the length of the interferometer l is much greater, the required monochromaticity can be reduced. When the distance between the source and prism is 100 m, and l is 100 m, for example, the $\Delta E/E$ required for fringe observation is only 1/50 for measuring a source size of $20 \mu\text{m}$ at an x-ray wavelength of 1 Å. The natural monochromaticity of undulator radiation is $1/N$, where N is the number of magnetic periods. Therefore, if the appropriate conditions can be realized, it is possible to measure the spatial coherence of undulator radiation without monochromator. Compared with the intensity correlation

method,^{12,13} this is considered to be an advantage of the interferometry with prism optics.

This prism interferometer cannot be applied to extreme-ultraviolet radiation and soft x rays because of strong absorption. However, the prism interferometer is considered to be a robust method for measuring the degree of spatial coherence in hard x-ray regions. In comparison with Young's double slit methods³⁻⁶ and other interferometric methods,^{7,10,14} this method can be adapted to a wide energy region and a wide range of coherent area by simple rotation of a prism. In this method, most of the coherent flux can be used to determine the degree of coherence, and two-dimensional mapping of correlation can be observed. Therefore, higher efficiency is expected, and there is the possibility to distinguish defects or distortion of wavefront from the measured image. They are considered to be advantages of the prism interferometer.

ACKNOWLEDGMENTS

The author would like to express his appreciation to Dr. H. Takano, Dr. A. Takeuchi, and Dr. K. Uesugi for their help in preparing the experimental setup. This experiment was performed under the approval of the Japan Synchrotron Radiation Research Institute (JASRI) (Proposal No. 2002B0176).

- ¹Y. Suzuki, *Jpn. J. Appl. Phys., Part 2* **41**, L1019 (2002).
- ²Y. Kohmura, T. Ishikawa, H. Takano, and Y. Suzuki, *J. Appl. Phys.* **93**, 2283 (2003).
- ³S. Aoki and S. Kikuta, *Jpn. J. Appl. Phys.* **13**, 1385 (1974).
- ⁴C. Chang, P. Naulleau, E. Anderson, and D. Attwood, *Opt. Commun.* **182**, 25 (2000).
- ⁵D. Paterson, B. E. Allman, P. J. McMahon, J. Lin, N. Moldovan, K. A. Nugent, I. McNulty, C. T. Chantler, C. C. Retsch, T. H. Irving, and D. C. Mancini, *Opt. Commun.* **195**, 79 (2001).
- ⁶R. A. Bartels, A. Paul, M. M. Murnane, H. C. Kapteyn, S. Backus, Y. Liu, and D. T. Attwood, *Opt. Lett.* **27**, 707 (2002).
- ⁷V. Kohn, I. Snigireva, and A. Snigirev, *Phys. Rev. Lett.* **85**, 2745 (2000).
- ⁸H. Yamazaki and T. Ishikawa, *Proc. SPIE* **2856**, 279 (1996).
- ⁹Y. Kohmura, Y. Suzuki, M. Awaji, T. Tanaka, T. Hara, S. Goto, and T. Ishikawa, *Nucl. Instrum. Methods Phys. Res. A* **452**, 343 (2000).
- ¹⁰W. Cash, A. Shipley, S. Osterman, and M. Joy, *Nature (London)* **407**, 160 (2000).
- ¹¹A. R. Lang and A. P. W. Makepeace, *J. Synchrotron Radiat.* **6**, 59 (1999).
- ¹²E. Gluskin, E. E. Alp, I. McNulty, W. Sturhahn, and J. Sutter, *J. Synchrotron Radiat.* **6**, 1065 (1999).
- ¹³M. Yabashi, K. Tamasaku, and T. Ishikawa, *Phys. Rev. Lett.* **87**, 140 801 (2001).
- ¹⁴J. J. A. Lin, D. Paterson, A. G. Peele, P. J. McMahon, C. T. Chantler, K. A. Nugent, B. Lai, N. Moldovan, Z. Cai, D. C. Mancini, and I. McNulty, *Phys. Rev. Lett.* **90**, 074801 (2003).
- ¹⁵M. Born and E. Wolf, *Principles of Optics*, 6th ed. (Cambridge University Press, Cambridge, 1997), Chaps. 7 and 10.
- ¹⁶L. Mandel and E. Wolf, *Optical Coherence and Quantum Optics* (Cambridge University Press, Cambridge, 1995), Chap. 4.
- ¹⁷H. Takano, Y. Suzuki, K. Uesugi, A. Takeuchi, and N. Yagi, *Proc. SPIE* **4499**, 126 (2001).